atmosphere

MDPI

Supplementary Materials: Deconstructing global observed and reanalysis total cloud cover fields based on Pacific climate modes

Petru Vaideanu[1, 2], Monica Ionita[1, 3, 4], Mirela Voiculescu[5] , and Norel Rimbu[1]

The percentage of variance explained for all the spatial structures provided by the EOFs and the CCAs used in our study

Table S1. | The variances explained by each EOF pattern from ISPCC, PATMOS-x and ERA5R TCC data.

	ISPCC Explained variance	**PATMOS-x Explained variance**	**ERA5R Explained variance**
EOF 1	24 %	23 %	19.1 %
EOF 2	11 %	9 %	9.6 %
EOF 3	5 %	4%	7.1 %
EOF 4	4 %	4%	4.5 %
EOF 5	4 %	3%	3.4 %
EOF 6	3 %	2%	2.9 %
EOF 7	3 %	2%	2.3 %
EOF 8	2 %	2%	2.1 %

Table S2. | The variances explained by each TCC pattern obtained through the CCA time using ISPCC PATMOS-x, and ERA5R TCC data.

CCA	**Explained variance TCC ISPCC**	**Explained variance TCC PATMOS-x**	**Explained variance TCC ERA5R**
CCA Pair1	5 %	5 %	4 %
CCA Pair2	4 %	4 %	5 %
CCA Pair3	19 %	17 %	13 %
CCA Pair4	7 %	8%	6 %
CCA Pair5	4 %	3 %	7 %

CCA Pair7	4 %	2 %	3 %
CCA Pair7	3 %	4 %	3 %
CCA Pair8	3 %	4 %	2 %

Comparison between the ISPCC and PATMOS-x datasets with regards to regional TCC impact induced by the EP and the CP ENSO

The global cloud structures associated with the EP ENSO and the CP ENSO) are similar over most of the regions, but differences between the results obtained using the ISPCC and the PATMOS-x data are observed over parts of Australia, North America and South America. In order to assess the robustness of these differences among both datasets, we performed an EOF analysis on both cloud cover data restricted to 120°E - 80°W, 10°S - 10°N region and we regressed the ISPCC and PATMOS-x cloud data on the two associated PC's, with results shown in Fig. S2. The regression maps associated to the EP ENSO (Fig S2, a and b) are virtually identical with the ones from the CCA pair linked to this climate mode). It has been shown that El-Niño events generate an increase in precipitation over the south-eastern part of North America (Chiodi and Harrison, 2013), the south of California (Jong et al., 2016) and the south-eastern part of South America (Garreaud et al., 2009). Over most of Australia (King et al., 2015) and the north-eastern part of South America (Sulca et al., 2018), El-Niño events generate a decrease in precipitation. These regional features regional features are better captured by the global TCC structure obtained using the PATMOS-x data. Also, the regression maps obtained using the PATMOS-x data (Supp. Fig 2, b) include an increase in cloudiness in the north-western part of South America, which has been only recently identified (Sulca et at., 2018) and is not captured in the regression map obtained using ISPCC data. Also, the areas where the statistical significance is over 95 % are more extended in the spatial structure obtained using the PATMOS-x data.

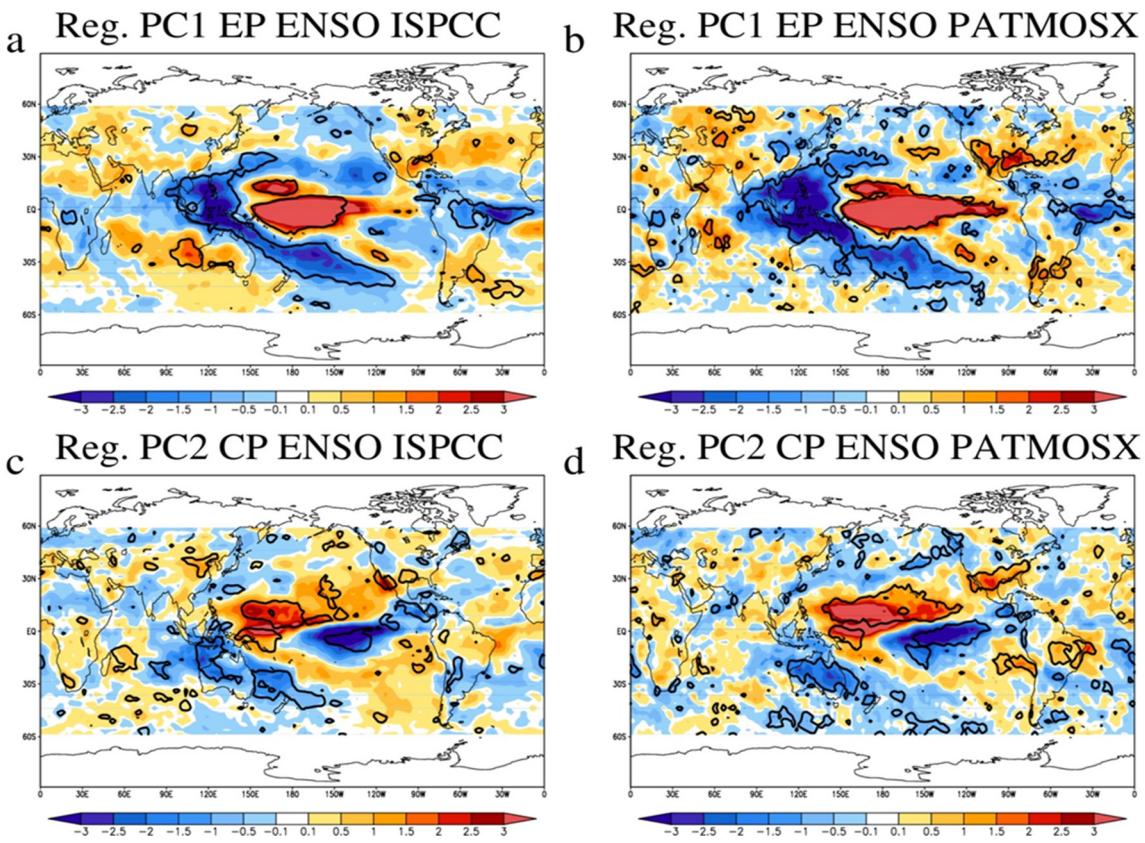

Figure S1. | ***Regression maps*** of ISPCC (a, c) ((std. dev/ %) and PATMOS-x (b, d) (std. dev/%) fields on the time series of the Tropical Pacific EOF structure associated to the EP ENSO (a, b) and the CP ENSO (c, d). The associated statistical significance in the highlighted areas is above 9.5 %.

Supporting the robustness of the methodology used to remove the trend from SST and TCC data used in this study.

Similar results are obtained if the warming trend is not removed from the SST field (Fig. S2), or from the ERA5R TCC data (Fig. S3). This is not surprisingly, since neither of the two ENSO modes analysed in this study exhibits a trend.

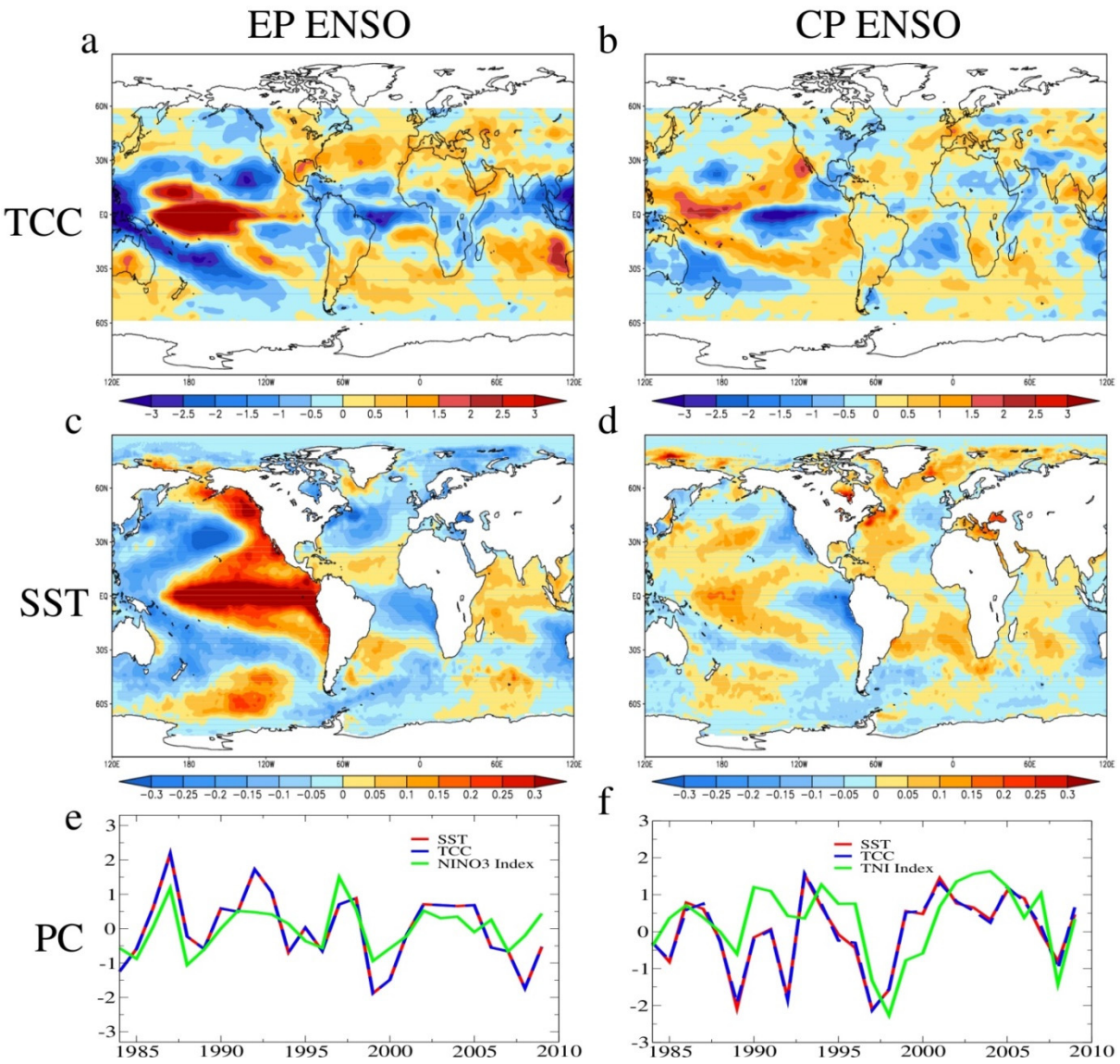

Figure S2. | The EP ENSO (left) and the CP ENSO (right) footprints on total cloud cover identified without removing the trend from HadISST data.

Left column: The third most coupled TCC (%) -SST (°C) pair identified through CCA using ISPCC data: the TCC pattern (a), explaining 10 % of variance, the SST structure (c), explaining 8 % of variance and the associated time series (e) with TCC (blue line), SST (red line) and Nino3 Index (green line). Their correlation coefficient is 0.99 and the correlation with NINO3 Index is 0.80.

Right column: The fourth coupled TCC (%) -SST (°C) pair identified through CCA using ISPCC data: the TCC pattern (b), explaining 9 % of variance, the SST structure (d), explaining 7 % of variance and the associated time series (f) with TCC (blue line), SST (red line) and TNI Index.

Chiodi, A. M. and Harrison, D. E.: El Niño impacts on seasonal US atmospheric circulation, temperature, and precipitation anomalies: the OLR-event perspective, J Climate, 26, 822–37, https://doi.org/10.1175/JCLI-D-14-00387.1, 2013.

Garreaud, R.D., Vuille, M., Compagnucci, R., Marengo, J. Present-day South American climate. Palaeogeogr., Palaeoclimatol., Palaeoecol., 281, 180-195, doi: 10.1016/j.palaeo.2007.10.032, 2009

Jeong, H. and Ahn, J.: A new method to classify ENSO events into eastern and central Pacific types, Int J Climatol, 37, 2193-2199, https://doi.org/10.1002/joc.4813, 2016.

King, A.D., Markus, G., Donat, M.G., Alexander, L,V., Karoly, D.J. The ENSOAustralian rainfall teleconnection in reanalysis and CMIP5. 44:2623–2635. doi:10.1007/s00382-014-215, 2015

Sulca, J., Takahashi, K., Espinoza, J.C., Vuille, M. and Lavado-Casimiro, W., Impacts of different ENSO flavors and tropical Pacific convection variability (ITCZ, SPCZ) on austral summer rainfall in South America, with a focus on Peru. Int. J. Climatol. doi:10.1002/joc.5185, 2018